

INTERFEROMETRIC CO OBSERVATIONS OF SUBMILLIMETER-FAINT, RADIO-SELECTED STARBURST GALAXIES AT $z \sim 2$

S. C. CHAPMAN,^{1,2} R. NERI,³ F. BERTOLDI,⁴ IAN SMAIL,⁵ T. R. GREVE,⁶ D. TRETHERWEY,¹ A. W. BLAIN,⁷ P. COX,³
R. GENZEL,⁸ R. J. IVISON,^{9,10} A. KOVACS,⁴ A. OMONT,¹¹ AND A. M. SWINBANK⁵

Received 2008 February 27; accepted 2008 July 22

ABSTRACT

High-redshift, dust-obscured galaxies, selected to be luminous in the radio but relatively faint at $850 \mu\text{m}$, appear to represent a different population from the ultraluminous submillimeter-bright population. They may be star-forming galaxies with hotter dust temperatures, or they may have lower far-infrared luminosities and larger contributions from obscured active galactic nuclei (AGNs). Here we present observations of three $z \sim 2$ examples of this population, which we term “submillimeter-faint radio galaxies” (SFRGs; RG J163655, RG J131236, and RG J123711) in CO(3–2) using the IRAM Plateau de Bure Interferometer to study their gas and dynamical properties. We estimate the molecular gas mass in each of the three SFRGs (8.3×10^9 , $<5.6 \times 10^9$, and $15.4 \times 10^9 M_\odot$, respectively) and, in the case of RG J163655, a dynamical mass by measurement of the width of the CO(3–2) line ($8 \times 10^{10} \text{ csc}^2 i M_\odot$). While these gas masses are substantial, on average they are 4 times lower than submillimeter-selected galaxies (SMGs). Radio-inferred star formation rates ($\langle \text{SFR}_{\text{radio}} \rangle = 970 M_\odot \text{ yr}^{-1}$) suggest much higher star formation efficiencies than are found for SMGs and shorter gas depletion timescales (~ 11 Myr), much shorter than the time required to form their current stellar masses (~ 160 Myr; $\sim 10^{11} M_\odot$). By contrast, star formation rates (SFRs) may be overestimated by factors of a few, bringing the efficiencies in line with those typically measured for other ultraluminous star-forming galaxies and suggesting that SFRGs are more like ultraviolet-selected (UV-selected) star-forming galaxies with enhanced radio emission. A tentative detection of RG J163655 at $350 \mu\text{m}$ suggests hotter dust temperatures, and thus gas-to-dust mass fractions, similar to the SMGs.

Subject headings: cosmology: observations — galaxies: evolution — galaxies: formation —
galaxies: high-redshift — galaxies: starburst

Online material: color figures

1. INTRODUCTION

Submillimeter surveys have provided an efficient probe of star formation activity in ultraluminous infrared (IR) galaxies (ULIRGs; $>10^{12} L_\odot$) in the distant universe (e.g., Smail et al. 1997; Hughes et al. 1998; Barger et al. 1998; Blain et al. 2002; Chapman et al. 2002), with bright submillimeter emission providing unambiguous evidence of massive quantities of dust, heated predominantly by young stars rather than AGNs (e.g., Chapman et al. 2003a; Alexander et al. 2005; Menendez-Delmestre et al. 2007; Valiante et al. 2007; Pope et al. 2008). Before the availability of the Atacama Large Millimeter Array (ALMA), confusion will continue to limit the sensitivity of current submillimeter surveys. As a result, many ULIRGs fall below the detection limits due to variations in their spectral energy distributions (SEDs), usually parameterized in terms of dust

temperature (T_d), meaning that entire populations of star-forming galaxies may have been missed by submillimeter surveys.

For a fixed far-infrared luminosity (FIR), a galaxy with a higher T_d will be weaker in the submillimeter at $850 \mu\text{m}$ than a galaxy with a lower T_d . Specifically, raising T_d from the canonical ~ 35 K for SMGs to 45 K will result in a factor of ~ 10 drop in $850 \mu\text{m}$ flux density (Blain 1999; Chapman et al. 2000, 2004b). These galaxies should, however, be accessible in the radio wave band, regardless of their specific SEDs, since the radio correlates with the integrated FIR emission (Helou et al. 1985) with a small ~ 0.2 dex dispersion and no observable dependence on SED type. However, there is potential for large AGN contaminations in the radio, as has often been the case with mid-IR selection of $z > 1$ ULIRGs (e.g., Houck et al. 2005; Yan et al. 2005, 2007; Sajina et al. 2008; Weedman et al. 2006a, 2006b; Desai et al. 2006), and the facilities required to provide the high-resolution, multifrequency radio data needed to decontaminate the samples (e.g., Ivison et al. 2007a) are not yet available.

Substantial populations of apparently star-forming galaxies at $z \sim 2$ have been uncovered through deep 1.4 GHz radio continuum observations, many of which are not detected at submillimeter wavelengths with the current generation of instruments (Barger et al. 2000; Chapman et al. 2001, 2003b, 2004a [hereafter C04]). That these galaxies are luminous in the radio and spectroscopy suggests that star formation is powering their bolometric output (there is little or no sign of high-ionization emission lines, characteristic of AGNs in their UV/optical spectra). These galaxies could, in principle, span a range in properties from deeply obscured AGNs to far-IR-luminous starbursts. In the latter case, one would expect a different SED from a typical SMG, a

¹ Institute of Astronomy, Madingley Road, Cambridge, CB3 0HA, UK.

² University of Victoria, Victoria, BC, V8W 3P6, Canada.

³ Institut de Radio Astronomie Millimétrique (IRAM), St. Martin d’Hères, France.

⁴ Max-Planck Institut für Radioastronomie (MPIfR), Bonn, Germany.

⁵ Institute for Computational Cosmology, Durham University, South Road, Durham DH1 3LE, UK.

⁶ Astronomy Department, Max-Planck Institut für Astronomie, Königstuhl-17, D-69117, Heidelberg, Germany.

⁷ California Institute of Technology, Pasadena, CA 91125.

⁸ Max-Planck Institut für extraterrestrische Physik (MPE), Garching, Germany.

⁹ UK Astronomy Technology Centre, Royal Observatory, Blackford Hill, Edinburgh EH9 3HJ, UK.

¹⁰ Institute for Astronomy, University of Edinburgh, Royal Observatory, Blackford Hill, Edinburgh EH9 3HJ, UK.

¹¹ Institut d’Astrophysique de Paris, CNRS, Université de Paris, Paris, France.

TABLE 1
PROPERTIES OF CO-OBSERVED SFRGs

R.A.	Decl.	$z(\text{CO})$	$z(\text{UV})$	$z(\text{H}\alpha)$	$L_{\text{FIR, radio}}$ ($10^{12} L_{\odot}$)	T_d (K)	S_{CO} (Jy km s $^{-1}$)	L'_{CO} (10^{10} K km s $^{-1}$ pc 2)	FWHM_{CO} (km s $^{-1}$)	M_{dyn} ($10^{10} M_{\odot}$)	M_{gas} ($10^9 M_{\odot}$)
16 36 55.04.....	41 04 32.0	2.189	2.186	2.192	7.1 ± 0.9	>46	0.34 ± 0.07	1.04 ± 0.21	410 ± 40	$8.4 \sin^2 i$	8.3 ± 1.7
13 12 36.01.....	42 40 44.1	...	2.240	2.243	6.7 ± 0.6	>48	<0.27 ^a	<0.71	<5.6
12 37 11.34.....	62 32 31.0	~ 1.996	...	1.996	16.7 ± 0.7	>45	0.70 ± 0.22	1.93 ± 0.60	15.4 ± 4.8

^a For RG J131236, we set a limit for a 500 km s $^{-1}$ FWHM line centered at the H α redshift.

higher T_d , for instance. These submillimeter-faint radio sources have a large volume density at $z \sim 2$, even larger than the SMGs (Haarsma & Partridge 1998; Richards et al. 1999; Chapman et al. 2003a; C04; Barger et al. 2007). There are $\rho = 2 \times 10^{-5}$ Mpc $^{-3}$ radio sources with $L_{1.4 \text{ GHz}} > 10^{31}$ ergs s $^{-1}$ Hz $^{-1}$ at $z \sim 2$ compared with $\rho = (6.2 \pm 2.3) \times 10^{-6}$ Mpc $^{-3}$ for SMGs brighter than 5 mJy at 850 μm at the same epoch (Chapman et al. 2003b, 2005). As essentially all of these SMGs form a subset of these radio sources (Chapman et al. 2005; Pope et al. 2006; cf. Ivison et al. 2002), this implies that $\sim 14 \times 10^{-6}$ Mpc $^{-3}$ luminous radio sources remain undetected at submillimeter wavelengths. Understanding the exact properties of these galaxies is therefore of great importance. If they are all forming stars at the rates implied by their radio luminosities, they would triple the observed star formation rate (SFR) density (SFRD) at $z \sim 2$. By contrast, if their radio luminosity comes from a mix of star formation and AGNs, they have less impact on the global SFRD, but they increase the highly obscured AGN fraction at these epochs (e.g., Daddi et al. 2007a; Casey et al. 2008b) and contribute substantially to black hole growth.

Together with other observations, the redshifted cooling emission lines of CO allow us to assess and compare the energy source of SFRGs with that of SMGs and other distant star-forming galaxies via measurements of their gas and dynamical masses. In this paper, we present the results of a pilot study with the IRAM Plateau de Bure Interferometer (PdBI) to detect molecular gas in SFRGs through the rotational CO(3–2) line emission. In § 2 we describe the sample properties and observations, both with PdBI and other facilities. Section 3 presents the CO(3–2) detections and limits obtained from the PdBI observations, § 4.1 estimates gas properties, star formation rates and efficiencies, and § 4.2 compares the SFRGs to other galaxy populations. Finally, § 5 discusses the results and places them in a broader galaxy evolution context. Throughout, we assume a cosmology with $h = 0.7$, $\Omega_{\Lambda} = 0.72$, and $\Omega_M = 0.28$ (e.g., Hinshaw et al. 2008).

2. SAMPLE PROPERTIES AND OBSERVATIONS

Our sample is drawn from an expansion of the C04 submillimeter-faint, radio-selected galaxy (SFRG) program, with galaxies drawn from several deep radio survey fields with typical sensitivity limits of $\sigma = 4\text{--}8$ μJy (e.g., Biggs & Ivison 2006). In the submillimeter, the survey fields are imaged to a typical depth

of $\sigma_{850 \mu\text{m}} \sim 1\text{--}2$ mJy (e.g., Scott et al. 2002; Borys et al. 2003). We selected sources with redshifts, radio luminosities, and submillimeter limits typical of the population, $\langle z \rangle = 2.1$, $\langle L_{1.4 \text{ GHz}} \rangle = 2 \times 10^{31}$ ergs s $^{-1}$ Hz $^{-1}$, $L_{850 \mu\text{m}} < 1 \times 10^{31}$ ergs s $^{-1}$ Hz $^{-1}$ (< 2 mJy for $z \sim 2$) at the $\sim 2 \sigma$ level, lying within $\pm 1 \sigma$ of the median SFRG in (C04), and observed RG J163655 and RG J131236 based on suitability of R.A. and confidence in the optical spectroscopic redshifts. A third source from our sample, RG J123711, was observed previously with PdBI in the same field as an SMG, and we include this object here. We note that while the neighboring SMG (SMM J123712.0+621326) lies only 8'' to the southeast, we are confident that RG J123711 is not a luminous submillimeter emitter. First, SMM J123712, has a strong CO line detection (I. Smail et al. 2008, in preparation) with a $\sim 5 \sigma$ detection $S_{\text{CO}(3-2)} = 1.2$ Jy km s $^{-1}$, comparable to typical SMGs from Greve et al. (2005). Second, the 850 μm emission peak (with a $R = 7''$ beam) in our Submillimeter Common-User Bolometer Array (SCUBA) map is centered on the radio source position, whereas no significant peak is observed at the position of RG J123711. Removing a 850 μm point source from the position of SMM J123712 reveals an even lower 850 μm flux density (0.1 ± 1.2 mJy) at the position of RG J123711 than the 2.2 ± 1.2 mJy conservatively adopted for our calculations (Table 2). Importantly, the small 850 $\mu\text{m}/1.4$ GHz flux ratio for this source is clearly comparable to SFRGs, not to the typical radio-detected SMGs in Chapman et al. (2005) or Ivison et al. (2007b). The properties of these SFRGs are listed in Tables 1 and 2, and displayed in Figures 1 and 2.

2.1. PdBI Observations

RG J163655 and RG J131236 were observed in their redshifted CO(3–2) lines and in the continuum at ~ 108 GHz using the newly refurbished PdBI receivers for 11.5 and 4.8 hr, respectively. Observations were made in D configuration on 2007 January 24, April 28, May 8 and June 3, with good atmospheric phase stability (seeing 0.7''–1.4'') and reasonable transparency (0.5 mm of precipitable water vapor). For RG J163655, the H α redshift showed a considerable offset from that inferred from UV absorption and emission lines. While this was conceivably due to a large-velocity starburst wind (~ 1300 km s $^{-1}$), we considered the possibility that one redshift might have calibration or resolution problems. We therefore observed RG J163655 split over

TABLE 2
PHOTOMETRIC PROPERTIES OF SFRGs

Source	20 cm (μJy)	850 μm (mJy)	350 μm (mJy)	24 μm (μJy)	8.0 μm (μJy)	5.8 μm (μJy)	4.5 μm (μJy)	3.6 μm (μJy)	I (AB mag)	R (AB mag)
RG J163655.....	43.9 ± 7.1	-1.5 ± 1.1	13.7 ± 6.9	<150	14.4 ± 2.7	16.8 ± 3.5	11.9 ± 1.1	9.9 ± 0.7	23.5	23.8
RG J131236.....	48.7 ± 4.1	0.4 ± 1.1	8.4 ± 2.7	<11	7.0 ± 1.1	5.4 ± 0.7	24.2	25.0
RG J123711.....	133.1 ± 5.1	2.2 ± 1.2	...	531 ± 8	37.5 ± 0.8	42.1 ± 1.2	35.8 ± 0.3	32.3 ± 0.2	24.9	25.8

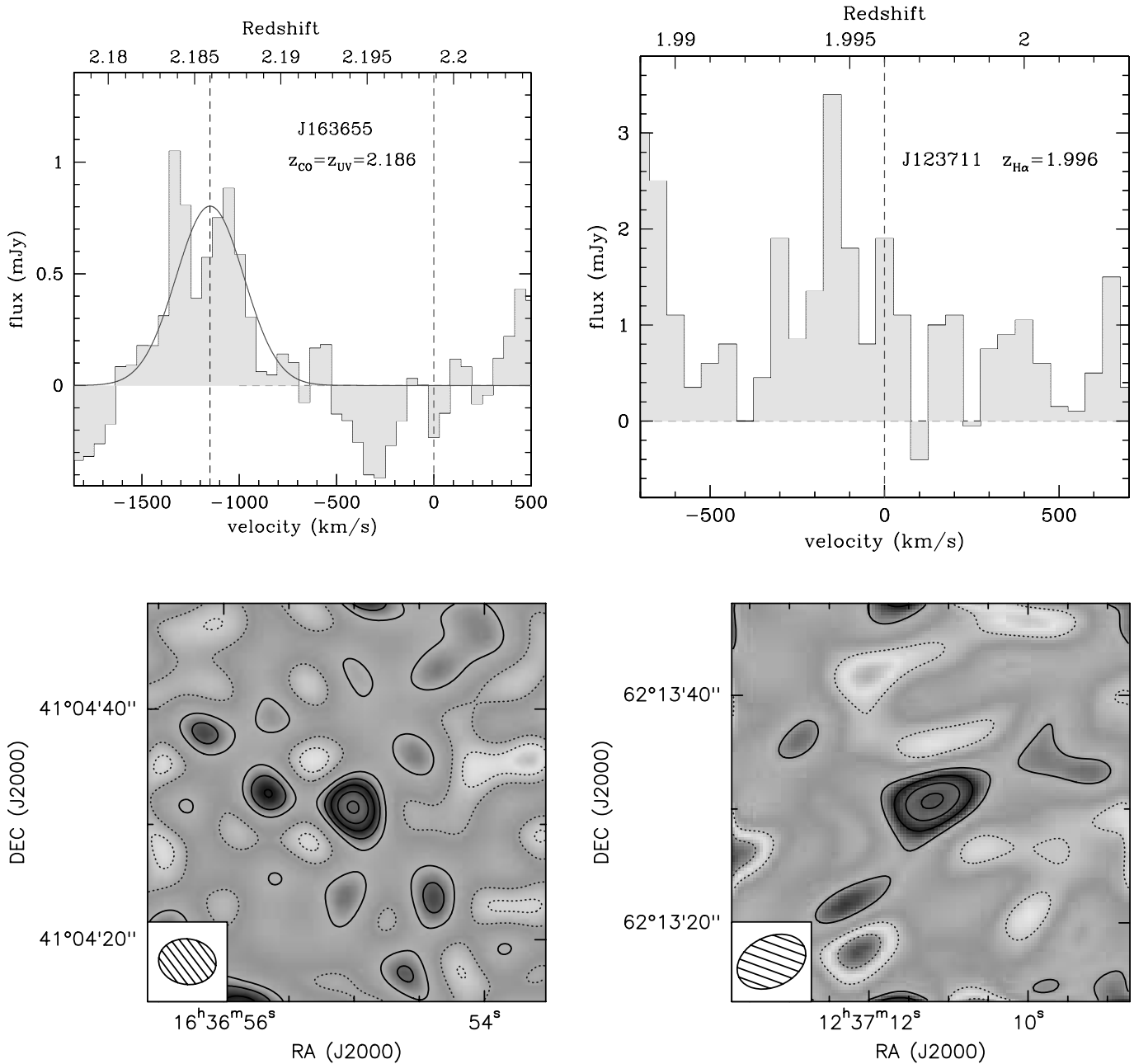


FIG. 1.—*Top*: CO(3–2) spectra for the two candidate detections. The spectra are shown smoothed with a 50 km s^{-1} boxcar filter and with respect to the zero-velocity offsets defined from the $\text{H}\alpha$ emission-line redshift (red dashed line). The best-fit Gaussian profile is shown for the emission line in RG J163655, along with the UV-inferred redshift from interstellar absorption lines (blue dashed line). *Bottom*: Velocity-averaged spatial maps of CO emission, from -1500 to -800 km s^{-1} (RG J163655), where contours are from -1 to 5σ in steps of σ ($0.05 \text{ mJy beam}^{-1}$). RG J123711 does not represent a formal CO detection. We measure a significance of 3.2σ integrating over the full band. The field of view, on a side, is $35''$, with the size of the beam shown to the top left. Both CO emitters lie exactly at the radio source position to within $1''$. [See the electronic edition of the Journal for a color version of this figure.]

two slightly offset frequency settings to span all measured redshifts. The overall flux scale for each observing epoch was calibrated using a variety of sources. In each observing epoch, between three and six sources were used. The visibilities were resampled to a velocity resolution of 55 km s^{-1} (20 MHz), providing 1σ line sensitivities of $1.6 \text{ mJy beam}^{-1}$. The corresponding synthesized beam, adopting natural weighting, was similar for both sources, $5.0''$ by $4.0''$ at P.A. $\sim 80^\circ$, east of north.

RG J123711 was previously observed at PdBI in a field with an SMG at the phase center (SMM J123712) in the program described by Neri et al. (2003) and Greve et al. (2005) using a previous generation of receivers. Observations proceeded sim-

ilarly to those described by Greve et al. (2005). The PdBI data for all three SFRGs were calibrated, mapped, and analyzed using the GILDAS software package. The CO(3–2) spectra and images of the two candidate SFRG detections, RG J163655 and RG J123711, are shown in Figure 1. *Spitzer* observations of the SFRGs in this paper were taken with the Infrared Array Camera (IRAC) and the Multiband Imaging Photometer (MIPS) through various GTO and Legacy programs.

2.2. Other Observations

RG J163655.—In addition to the SCUBA $850 \mu\text{m}$ photometry, observations were obtained at $350 \mu\text{m}$ with the SHARC2 camera

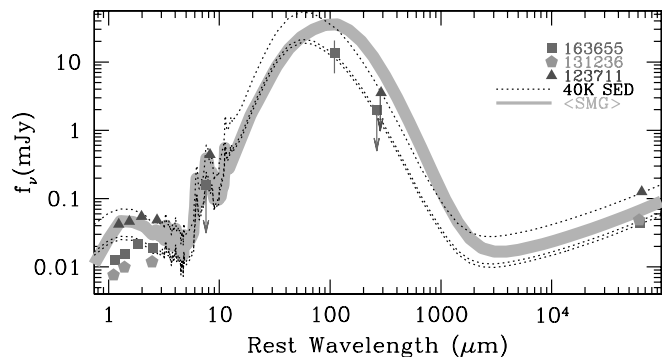


FIG. 2.—SEDs for RG J163655, RG J131236, and RG J123711. A local galaxy SED with $T_d = 40$ K (from Dale et al. 2001) is shown, normalized to the radio point in each case. An average fit to the SEDs of representative SMGs is shown as a heavy line (Chapman et al. 2005; Kovacs et al. 2006; Hainline et al. 2008). [See the electronic edition of the Journal for a color version of this figure.]

(Dowell et al. 2003) on the Caltech Submillimeter Observatory as part of the imaging campaign of Kovacs et al. (2006), where observational details can be found. A near-IR spectrum from the United Kingdom Infrared Telescope (UKIRT) UIST covering the $H\alpha/[N II]$ region (Swinbank et al. 2006) finds a large $H\alpha/[N II]$ ratio suggestive of a relatively low metallicity, $[Fe/H] \sim -0.9$, and no strong AGN component. While the $[O III] \lambda 500.7$ region was also covered with the instrument, we did not clearly detect any emission lines, setting a limit on the $[O III] \lambda 500.7$ line of $3.75 \times 10^{-17} \text{ W m}^{-2}$, again suggesting that an AGN does not dominate the energetics of this galaxy. The line width of the $H\alpha$ emission ($\text{FWHM}_{\text{rest}}$) is $420 \pm 100 \text{ km s}^{-1}$, and the integrated line flux of $5.0 \times 10^{-19} \text{ W m}^{-2}$ then suggests a SFR uncorrected for dust extinction of $150 \pm 50 M_{\odot} \text{ yr}^{-1}$ (Kennicutt 1998). The 1.4 GHz radio emission was unresolved by the Very Large Array (VLA) in its A configuration (Biggs & Ivison 2006). A relatively compact UV morphology is observed in the *Hubble Space Telescope* imaging, with $R_{1/2} = 0.25''$ (Swinbank et al. 2006).

RG J131236.—In C04, the optical (rest-frame UV) spectrum was presented, showing $Ly\alpha$ in emission, but all other detectable lines in absorption, and was classified as a pure starburst. The near-IR spectrum of RG J131236 from Keck NIRSPEC covering the $H\alpha/[N II]$ region (Swinbank et al. 2004) again finds a large $H\alpha/[N II]$ ratio suggestive of a low metallicity, $[Fe/H] \sim -0.9$. The line width of the $H\alpha$ emission is $450 \pm 220 \text{ km s}^{-1}$, and the integrated line flux of $(2.3 \pm 1.2) \times 10^{-19} \text{ W m}^{-2}$ then suggests an SFR uncorrected for dust extinction of $110 \pm 40 M_{\odot} \text{ yr}^{-1}$. The radio emission was unresolved by the VLA. Only ground-based imaging exists for this SFRG, showing a faint, unresolved source in $0.8''$ seeing.

RG J123711.—An X-ray detection and obscured AGN classification due to its X-ray luminosity by Alexander et al. (2005) contrasts a polycyclic aromatic hydrocarbon (PAH)-dominated mid-IR spectrum obtained by Pope et al. (2008) showing no obvious AGN component. No rest-frame UV spectrum for RG J123711 has been published, as there are no detected features. The redshift is based entirely on the near-IR spectrum where RG J123711 was detected with Keck NIRSPEC (Swinbank et al. 2004), once again finding a large $H\alpha/[N II]$ ratio suggestive of an $[Fe/H] \sim -0.8$. The narrow line width of the $H\alpha$ emission ($112 \pm 45 \text{ km s}^{-1}$) and the integrated line flux of $(0.4 \pm 0.3) \times 10^{-19} \text{ W m}^{-2}$ suggests an SFR uncorrected for dust extinction of $16 \pm 9 M_{\odot} \text{ yr}^{-1}$. Radio imaging of this SFRG with MERLIN ($0.3''$ synthesized beam; Casey et al. 2008b) reveals a double source structure with a $\sim 1''$ elongated feature and a relatively compact $R_{1/2} = 0.4''$ component.

3. RESULTS

The velocity-integrated line fluxes or limits for all three SFRGs are listed in Table 1. For RG J163655, inspection of the data cube shows a significant 4.9σ detection of CO(3–2) line emission at the phase center, integrated over the velocity channels at $\sim -1000 \text{ km s}^{-1}$ with a velocity width of 400 km s^{-1} FWHM. Fitting a Gaussian profile to the CO spectrum, we derive a best-fit redshift for the CO(3–2) emission of $z = 2.1859 \pm 0.0002$ and estimate the CO flux by summing the channels from -2 to $+2 \sigma$ of Gaussian fit to the line. We note that no significant continuum emission is detected from the line-free region ($\sim 650 \text{ MHz}$ of bandwidth) down to a 1σ sensitivity of $0.07 \text{ mJy beam}^{-1}$, consistent with the submillimeter limit, assuming a dust spectral index, $\nu^{+3.5}$, for a modified blackbody with emissivity, $\beta = +1.5$. For RG J131236, no significant emission is observed at the phase center, although the limit on the CO gas mass is still of great interest relative to the SMGs. For RG J123711, we tentatively detected (3.2σ) a positive signal integrated over the full band from -600 to $+600 \text{ km s}^{-1}$, centered on the $H\alpha$ -determined redshift of $z = 1.996$. A precise CO redshift cannot be determined for RG J123711, as the line shape cannot be determined in the low signal-to-noise (S/N) radio spectrum. To assess the possibility that we have simply detected continuum in this source, we analyze the radio spectral index, measured to be steep from the 8.4 GHz/1.4 GHz flux ratio (Muxlow et al. 2005), $S_{\nu} \propto \nu^{-0.69}$, and the synchrotron contribution at $\sim 3 \text{ mm}$ is negligible. This does not, however, preclude a contribution from an AGN component with the opposite spectral slope emerging at higher frequencies. It is clear that the full radio spectrum is needed to explore this issue, as well as the possibility of an obscured AGN.

In RG J163655, the CO-inferred redshift is close to the redshift measured from various interstellar absorption lines in the Keck LRIS UV spectrum, but is blueshifted by 1100 km s^{-1} from the $H\alpha$ line detected by Swinbank et al. (2006). Reanalysis of the near-IR spectrum does not significantly change the result, as the sky line calibrations appear to be as presented in Swinbank et al. (2006). If the detected line were dominated by $[N II]$ with $H\alpha/[N II] < 1$ —and we stress that there is no evidence in the spectrum of this—then the implied velocity offset would be $\sim 800 \text{ km s}^{-1}$, somewhat closer to the average CO velocity and consistent with the higher velocity peak in the detected CO profile. We cannot attribute the CO emission to an offset companion (as was the case for SMG J09431 in Tacconi et al. 2006), as the CO centroid is exactly at the near-IR and radio position to within the $1''$ centroiding uncertainty [$\sim \text{beam size} \times (S/N)^{-1}$]. The $H\alpha$ -inferred redshift has not always been representative of the CO redshift in SMG surveys (the average CO– $H\alpha$ offset is 150 km s^{-1}), presumably because the luminous core is so deeply dust enshrouded that wind outflows or satellite $H II$ regions are more strongly detected in $H\alpha$. We therefore put forward the hypothesis that we are detecting a highly dust-obscured gas-rich galaxy in CO(3–2), either a companion seen in projection or else one not well sampled by the $H\alpha$ observations. The rest-frame FWHM of the CO line is $376 \pm 40 \text{ km s}^{-1}$, close to that found in $H\alpha$ by Swinbank et al. (2006), but likely a coincidence, given that the CO and $H\alpha$ redshifts are discrepant.

The $350 \mu\text{m}$ SHARC-2 imaging of RG J163655 shows a tentative continuum detection, $S_{350 \mu\text{m}} = 2.4 \pm 6.5 \text{ mJy}$ at the radio position; however, given the telescope pointing errors and the low signal-to-noise (S/N) of any expected emission, we search a region comparable to the beam size ($9''$). A 2σ peak ($S_{350 \mu\text{m}} = 13.7 \pm 6.9 \text{ mJy}$) lies $7''$ from the radio position at $16^{\text{h}}36^{\text{m}}54.6^{\text{s}}, +41^{\circ}04'28''$ (J2000.0). Within this area there are

TABLE 3
DERIVED PROPERTIES OF THE SFRGs

Source	SFR _{radio} ($M_{\odot} \text{ yr}^{-1}$)	SFR _{UV} ($M_{\odot} \text{ yr}^{-1}$)	SFR _{Hα} ($M_{\odot} \text{ yr}^{-1}$)	SFR _{24 μm} ^a ($M_{\odot} \text{ yr}^{-1}$)	SFE ^b (L_{\odot}/M_{\odot})	Σ_{gas} ($M_{\odot} \text{ yr}^{-1} \text{ kpc}^{-2}$)	M^{*c} (M_{\odot})	Gas/Dust ^d	$\tau_{\text{depletion}}$ (Myr)	$\tau(\text{gas to stars})$ (Myr)
RG J163655	630 \pm 120	46 \pm 11	150 \pm 50	<255	600	70	1×10^{11}	52	13.2	160
RG J131236	610 \pm 91	33 \pm 16	110 \pm 40	...	<1450	<65	5×10^{10}	...	<9.2	80
RG J123711	1670 \pm 113	11 \pm 10	16 \pm 9	880 \pm 54	1330	35	4×10^{11}	100	9.2	240

^a SFR from 24 μm luminosity, assuming the average SED in Dale & Helou (2002).

^b Star formation efficiency (SFE) is the SFR divided by the molecular gas mass.

^c Stellar mass calculated as Borys et al. (2005), adopting their $L_K/M_{\odot} = 3.2$.

^d No limit is possible for RG J131236, since both gas and dust are limits.

only ~ 3 SHARC-2 beams and the chance of a spurious 2σ peak is only $\sim 6\%$. There is a high likelihood ($\sim 90\%$) that this peak is related to RG J163655, and this flux range is completely consistent with our SED fit to the radio photometry for RG J163655 (Fig. 2).

We calculate from the integrated CO(3–2) intensity (Jy km s^{-1}) the line luminosities and estimate the total cold gas masses ($\text{H}_2 + \text{He}$; listed in Table 1). We adopt $L'_{\text{CO}(3-2)} = 3.25 \times 10^7 S_{\text{CO}(3-2)} \nu_{\text{obs}}^{-2} (1+z)^{-3} D_L^2$, consistent with Solomon & Vanden Bout (2005).

We assume both a line luminosity ratio of $r_{32} = L'_{\text{CO}(3-2)}/L'_{\text{CO}(1-0)} = 1$ (i.e., a constant brightness temperature) and a CO-to- H_2 conversion factor of $\alpha = 0.8 M_{\odot} \text{ K km s}^{-1} \text{ pc}^2$. These values are appropriate for local galaxy populations exhibiting levels of star formation activity similar to our SFRGs (e.g., local ULIRGs; Solomon et al. 1997), and this choice also facilitates comparison with SMGs modeled with the same values (Greve et al. 2005). We discuss later how our conclusions would change if we adopted α and r_{32} values typical of the Milky Way.

3.1. Spitzer Properties of the SFRGs

All three SFRGs show a peaked SED in the mid-IR (Fig. 2), suggesting that this spectral region is dominated by stars rather than AGNs. These properties are used to derive the rest-frame K -band ($\sim 2.2 \mu\text{m}$) flux and convert to a stellar mass, in a manner similar to Borys et al. (2005), adopting their $L_K/M_{\odot} = 3.2$ characteristic of a burst with an age of ~ 250 Myr. We interpolated between IRAC bands to estimate $S_{2.2 \mu\text{m}}$ (Table 3).

3.2. Derived Properties

We then proceed to estimate various derived properties (listed in Table 3). Starting with the gas surface density, for RG J123711 we assume that the CO emission traces the same large, extended morphology ($>1''$ FWHM diameter) traced by resolved MERLIN radio imaging (see Casey et al. 2008b for details), suggesting a low gas surface density. For RG J163655 and RG J131236, neither the CO emission nor the VLA radio emission is resolved. Without information beyond the optical imaging described previously, we assume the gas in these two SFRGs is distributed in a disk with a radius similar to SMGs (e.g., Tacconi et al. 2008) of $R_{1/2} = 1.7 \text{ kpc}$ ($0.25''$), resulting in higher inferred gas surface densities. The CO luminosities for the three SFRGs are plotted as a function of FIR luminosity and compared to other high-redshift galaxies detected in CO in Figure 3.

A dynamical mass for the well-detected RG J163655 can be estimated by analyzing the CO line profile. We base our analysis on a single Gaussian fit to the line. CO emission is comparatively immune to the effects of obscuration and outflows and therefore provides an unbiased measurement of dynamics within the CO-emitting region. The line width of the CO emission ($410 \pm 40 \text{ km s}^{-1}$) implies a dynamical mass of $(8.4 \pm 2.1) \times 10^{10} \text{ csc}^2 i M_{\odot}$, as-

suming the gas lies in a disk with inclination i and a radius of $0.25''$ (1.7 kpc). Based on this, we calculate a gas-to-dynamical mass fraction of $f = M_{\text{gas}}/M_{\text{dyn}} \sim 0.10 \sin^2 i$. We note that the mean angle of randomly oriented disks with respect to the sky plane in three dimensions is $i = 30^\circ$ (Carilli & Wang 2006), resulting in an average inclination correction of $\text{csc}^2 i = 4$.

4. ANALYSIS

4.1. Star Formation Rate and Efficiency

The radio luminosity of the SFRGs forms our baseline estimate for the far-IR luminosity and SFRs (listed in Table 3), since we have only upper limits at 450 and 850 μm . We caution, however, that our flux-limited radio selection biases our sample to find objects of the same radio luminosity as SMGs, regardless of the origin of the radio power. There are clear examples within the wider SFRG sample in which AGNs dominate the radio power,

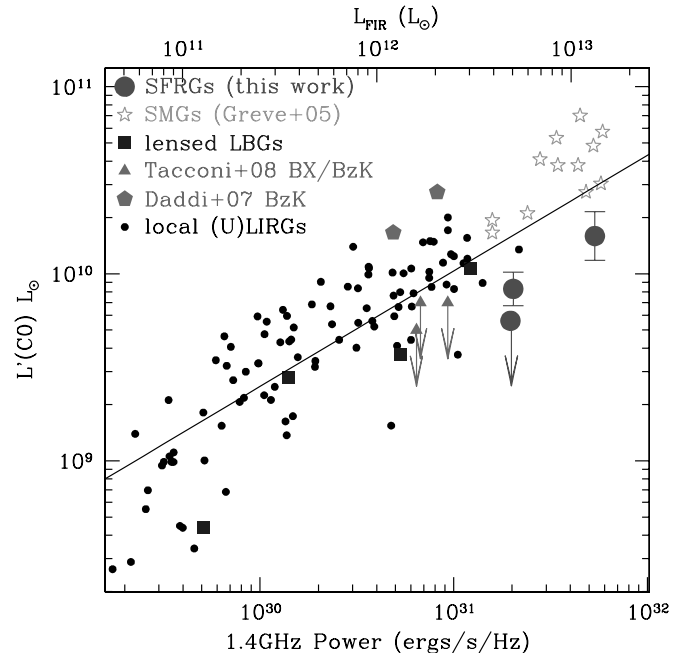


FIG. 3.— Comparison of the CO and radio luminosities for the three SFRGs described here, the SMGs from Greve et al. (2005) and Tacconi et al. (2006), the lensed LBGs detected in CO (Baker et al. 2004; Coppin et al. 2007; Kneib et al. 2005), the luminous $z \sim 2$ BX/BzK galaxies undetected in CO (Tacconi et al. 2008), and the two $z \sim 1.4$ BzK galaxies detected in CO by Daddi et al. (2008). The solid line is the best-fitting relation of the form $\log L'_{\text{CO}} = \alpha \log L_{\text{FIR}} + \beta$ to the local LIRGs and ULIRGs and the high-redshift SMGs from Greve et al. (2005); however, it is no longer quite the best fit when radio luminosity is considered consistently across the populations). With gas conversions fixed, the SFRGs appear to have lower CO gas masses than SMGs, although if the radio-inferred SFRs are overestimated, then the SFRGs could still lie on the plotted gas/SFR relation. [See the electronic edition of the Journal for a color version of this figure.]

despite an apparent starburst spectrum in the rest-frame UV (e.g., Casey et al. 2008a). The average $\langle \text{SFR}_{\text{radio}} \rangle = 970 M_{\odot} \text{ yr}^{-1}$, assuming the radio/FIR relation $q = \log(\text{FIR}/3.75 \times 10^{12} \text{ Hz})/S_{1.4 \text{ GHz}}$ (Helou et al. 1985), with $q = 2.34$ (Yun et al. 2001), a correction factor of 2.3 to total IR luminosity (TIR) appropriate for hotter dust SEDs (Dale & Helou 2002), and the conversion from Kennicutt (1998)

$$\text{SFR}(M_{\odot} \text{ yr}^{-1}) = 1.8 \times 10^{-10} L_{8-1000 \mu\text{m}}(L_{\odot}).$$

The SFRs from their dust-corrected rest-frame 1500 Å continuum flux are factors ~ 50 times less (as described in C04), and the UV emission is clearly not probing the true luminosities of these systems (Table 3). The $\text{H}\alpha$ emission line suggests SFRs (Table 3) 10 times less than the radio ($\langle \text{SFR}_{\text{H}\alpha} \rangle = 92$), although with the average extinction factor of $A_V \sim 2.9 \pm 0.5$ proposed for SMGs in Takata et al. (2006), this becomes $\langle \text{SFR}_{\text{H}\alpha, \text{corr}} \rangle = 1300 M_{\odot} \text{ yr}^{-1}$. This is consistent, on average, with the radio-inferred SFRs, although the individual radio/ $\text{H}\alpha_{\text{corr}}$ ratios show very poor correspondence. We have, of course, argued in the case of RG J163655 that the CO(3–2) and the $\text{H}\alpha$ line emission may be coming from distinct regions, so these arguments do not obviously apply in every case, and the average correction factor applied to the $L_{\text{H}\alpha}$ may not be appropriate either individually or for the population. The 24 μm fluxes (Table 2) would represent strong supporting evidence for large SFRs. We calculate $\text{SFR}_{24 \mu\text{m}}$ as in Pope et al. (2006) for consistency with SMGs (although strong 24 μm luminosities could also reveal a dominant hot AGN dust torus). In a large sample of SFRGs, the 24 μm luminosity distribution is indistinguishable from that of SMGs (Casey et al. 2008b). Two of our present three SFRGs have 24 μm observations, and only one is detected, the limit in the second case not being particularly constraining relative to the radio. The $\text{SFR}_{24 \mu\text{m}}$ (Table 3) could be consistent with the $\text{SFR}_{\text{radio}}$ given uncertainties in calibrating the SFR indicators.

For a reference point, which can be scaled through by uncertainties in the SFR, we adopt the $\text{SFR}_{\text{radio}}$ and calculate surface densities Σ_{SFR} and star formation efficiencies ($\text{SFE} = L_{\text{FIR}}/M_{\text{H}_2}$) for the SFRGs, using assumed sizes described previously and listed in Table 3. We find large star formation efficiencies (SFEs; 4 times larger than the SMGs on average), although the observational constraints on the SFRs for the SFRGs are consistent with having been overestimated by a factor of ~ 2 – 3 , which would bring them into reasonable agreement with the envelope of star formation efficiencies for SMGs, LBGs, and local ULIRGs.

We can also roughly estimate a lower limit to the gas-to-dust mass ratio where CO is detected (Table 3). We estimate similar dust mass limits for the SFRGs using

$$M_{\text{dust}}(M_{\odot}) = \frac{1}{1+z} \frac{S_{\text{obs}} D_L^2}{\kappa_d B(\nu_0, T_d)},$$

assuming $\kappa_{\nu} \propto \nu^{\beta}$, $\beta = +1.5$, and $B_{\nu}(T_d) \sim \nu^{+2}$ in the $M_{\text{dust}} < 1.6 \times 10^8 M_{\odot}$ from the 2σ limit on the 850 μm flux of $\sim 2.2 \text{ mJy}$ and assuming a dust mass absorption coefficient of $\kappa_{850 \mu\text{m}} = 0.15 \text{ m}^2 \text{ kg}^{-1}$. We find ratios of 50 and 100, with at least a factor of ~ 6 uncertainty accounting for our uncertainty of the dust temperature ($\Delta T_d \simeq \pm 5 \text{ K}$), dust emissivity coefficient ($\Delta \beta \simeq \pm 0.5$), and mass absorption coefficient (about a factor of ~ 3 ; e.g., Seaquist et al. 2004).

Assuming the molecular gas reservoirs we detect are fueling the star formation within these galaxies, then there is enough gas to sustain the current star formation for $\tau_{\text{depl}} \sim M(\text{H}_2)/\text{SFR}$, ranging from less than 9 to 13 Myr. Since we have also estimated

stellar masses, we can compare the gas depletion time with the time to form the current stellar mass of the system. At the current SFRs, $\tau_{\text{form}} \sim M_{\text{stars}}/\text{SFR}$ ranges from 80 to 240 Myr, which are comparable to the assumed ages of the stellar populations.

4.2. Comparison to Other Populations

Comparison of the SFRGs to the SMGs is of primary importance, since a major goal of the observations is to understand the degree to which SFRGs should be treated on a footing similar to SMGs in models and evolutionary calculations. Taking the average CO line luminosity and gas mass, we find intrinsic line luminosities a factor of ~ 4 lower than the median for SMGs (cf. $\langle L'_{\text{CO}} \rangle = (3.8 \pm 2.3) \times 10^{10} L_{\odot}$ and $\langle M_{\text{gas}} \rangle = (3.0 \pm 1.6) \times 10^{10} M_{\odot}$; Greve et al. 2005). The CO line width of RG J163655 is also much lower than the median of SMGs ($\langle \text{FWHM} \rangle = 780 \text{ km s}^{-1}$; Greve et al. 2005). Given that the CO-inferred gas masses are somewhat low compared to SMGs, we find, not surprisingly, that the gas depletion timescales are short compared to SMGs (which have $\tau_{\text{depl}} \sim 40 \text{ Myr}$; Greve et al. 2005), although the SFRGs are still within a physically plausible range. We have only a useful constraint on the size of the emitting region for RG J123711 to compare with higher resolution images of SMGs, although in general the SFRGs exhibit radio sizes and morphologies similar to SMGs (compare Chapman et al. [2004b] and Biggs & Ivison [2008] to Casey et al. [2008b]). The typical gas-to-dynamical mass fraction in SMGs is estimated to be ~ 0.3 , assuming a merger model (Greve et al. 2005), while they have SFEs of $L_{\text{FIR}}/M_{\text{H}_2} \sim 450 \pm 170 L_{\odot} M_{\odot}^{-1}$ (Greve et al. 2005), gas-to-dust mass ratios of ~ 200 (with a factor of a few uncertainty in the dust mass alone), and gas surface densities of $\sigma_{\text{gas}} \sim 3000 M_{\odot} \text{ yr}^{-1} \text{ pc}^2$ (Tacconi et al. 2006). Borys et al. (2005) estimate the average stellar mass for SMGs at $z > 1.5$ to be $3.2^{+3.4}_{-1.6} \times 10^{11} M_{\odot}$, slightly larger than the average $1.8 \times 10^{11} M_{\odot}$ for our three SFRGs.

Overall, this comparison suggests that SFRGs may be somewhat smaller mass objects (lower stellar mass, lower CO mass, and lower dynamical mass) than SMGs, but share with them a large radio luminosity. The SFRs of both SMGs and SFRGs are subject to sizable uncertainties, not least of which is the initial mass function (e.g., Baugh et al. 2005). Pope et al. (2006) have pointed out that SMG SFRs estimated from the 24 μm *Spitzer* MIPS observations are lower than those estimated from the 850 μm or radio wave bands, although this could represent an issue of relative calibrations of these indicators in this luminosity regime rather than intrinsic properties.

We can also compare the SFRGs to local populations and less luminous star-forming galaxies at $z \sim 2$. Locally, L'_{CO} increases with L_{FIR} for (U)LIRGs, with the Greve et al. (2005) sample of SMGs extending this trend out to the highest far-IR luminosities ($\gtrsim 10^{13} L_{\odot}$). For comparison, in Figure 3 we have plotted the SFRGs on the $L'_{\text{CO}}-L_{\text{FIR}}$ diagram, along with SMGs lying on the local relation, as well as three LBGs from the literature within the considerable uncertainties in their far-IR luminosities, three undetected BX/BzK galaxies (Tacconi et al. 2008), and two CO-detected BzK galaxies (Daddi et al. 2008; these sources lie above the relation). The SFRGs lie somewhat below this relation.

5. DISCUSSION

As our calculations above have shown, it is very difficult to estimate the precise gas masses for SFRGs due to various uncertainties. However, a potentially important result emerges from these CO observations: compared to SMGs, SFRGs appear to be significantly more efficient at producing stars from a given molecular gas mass. If this is strictly true, then SFRGs cannot be

interpreted as *scaled up* versions of local ULIRGs as Tacconi et al. (2006, 2008) have argued is the case for SMGs, since their gas masses appear to be lower than expected for their radio luminosities. There are two considerations to be taken into account here. First, the far-IR luminosities and thus SFRs may be overestimated from the radio, for instance, if buried AGNs were present. While none of these sources have AGN signatures in their UV or optical spectra, a deeply obscured AGN could still be driving a significant portion of the radio luminosity (e.g., Daddi et al. 2007b; Casey et al. 2008a). A further possible complication comes again from the radio selection of these objects. There is a ~ 0.25 dex scatter in the radio-FIR relation (Yun et al. 2001), and while locally there is no apparent correlation between SED shape and radio-FIR scaling, it is possible in our SFRGs that we are selecting galaxies that are among the lower 0.25 dex (weaker FIR per unit radio). If the SFRs in our galaxies were several times lower, then the efficiencies would be similar to the average SMG (Fig. 3). Second, the conversion from CO(3–2) to molecular gas mass may not be the same as for SMGs. If α_{CO} were greater than the ~ 1 estimated for local ULIRGs (and as inferred to be correct for SMGs), these SFRGs could make up the shortfall in molecular gas mass from the average SMG (~ 4 times), although the conversion would have to approach that typically adopted for the Milky Way, $\alpha_{\text{CO}} = 4.6$ (Solomon & Vanden Bout 2005). This is unlikely, given that the SFRGs often show clear evidence in high-resolution radio observations for merger-driven starbursts (Casey et al. 2008b).

It is noteworthy that while our observations have highlighted an ultraluminous $z \sim 2$ population that may build stars in an extremely efficient mode (or at least as efficient as SMGs if their SFRs are overestimated by factors of several), recent observations (Daddi et al. 2008) have identified a population of $z \sim 1.5$ galaxies that they detect in CO(2–1) exhibiting the opposite property, low-efficiency star formation. These Daddi et al. galaxies are selected as large massive disklike galaxies, and it is perhaps not surprising that they form stars in an apparently quiescent “spiral galaxy” mode. Nonetheless, it is intriguing that galaxies in the high-redshift universe have been discovered with such a wide range of star-forming efficiencies (from poor to extreme) all lying in the 10^{12} – $10^{13} L_{\odot}$ regime. Massive galaxies are being built in a variety of modes in the $z = 1$ – 3 peak star formation period.

The short depletion times compared to the long times to form the stellar masses suggest that we may be seeing SFRGs in the last phase of their current star formation episodes. However, one would expect on average to find SFRGs as a population halfway through their gas consumption lifetimes. In this context, the small ages imply either a very high duty cycle or that the SFRs are overestimated from the radio luminosity. We reiterate that the large FIR luminosity estimates for our SFRGs are based mainly on the radio/FIR relation, which apparently applies for SMGs (Kovacs et al. 2006), but is only marginally supported for SFRGs through the $24 \mu\text{m}$ luminosity and dust-corrected $\text{H}\alpha$ measurements. It is possible that we are overestimating their star formation activity, which would lead us to underestimate the duration timescales above.

We also note that the observed CO may be closely associated with the star formation and thus is probably warm and highly visible (i.e., with low α_{CO}). It does not rule out the existence of a cooler, less visible component (with high α_{CO}), not intimately associated with the current zone of star formation (e.g., in the inner disk) that may still become available within its own dynamical timescale to fuel star formation. The result above may therefore be affected by the selection for the highly visible component of the molecular gas.

In order to evaluate the implications of these results for massive galaxy formation, we recall that these three galaxies have characteristics typical of the SFRG population at all wavelengths measured. Our results underline the major role of gas consumption over short timescales and with high efficiencies, characterizing rapid and strong merger-driven bursts as a major growth mode for both stellar mass and black holes in the distant universe. Even if the SFRs in these SFRGs were overestimated by a factor of a few, they would remain ULIRG-class galaxies. If we assume that $\sim 50\%$ of the submillimeter-faint SFRGs at $z \sim 2$ are dominated by star formation at levels comparable to SMGs, we arrive at a density of $\sim 5 \times 10^{-6} \text{ Mpc}^{-3}$, similar to that observed for SMGs (Chapman et al. 2003b). Together, the SMGs and SFRGs represent a volume density 10 times smaller than measured for galaxies inferred to be forming stars at low efficiencies by Daddi et al. (2007b), which have space densities of order of 10^{-4} Mpc^{-3} . With SFRs a few to 10 times larger in the SMGs and SFRGs, the net effect is roughly equal numbers of stars being formed in both high- and low-efficiency modes at $z \sim 2$.

Further study should ascertain whether other SFRGs follow a pattern similar to the galaxies studied in this paper. A substantial sample will allow the properties of the gas-to-dynamical mass ratio to be determined accurately for the population, since we currently have only one well-detected line profile, and the dynamical mass determination is limited by the unknown inclination.

6. CONCLUSIONS

1. RG J163655 is a gas-rich star-forming system, with a tentative detection at $350 \mu\text{m}$ supporting the notion of a higher dust temperature than typical SMGs. RG J123711 is also likely to be a gas-rich system, although the CO detection is still tentative for this source. This system is further compromised because it lies only $8''$ from a known SMG. However, both the submillimeter map and our weak CO(3–2) detection with PdBI relative to the strong CO(3–2) detection of the neighboring SMG suggest that this radio source is not a bright submillimeter emitter. RG J131236, undetected in CO, is either offset in CO velocity from our 1500 km s^{-1} observing band or else is the weakest CO emitter of these three galaxies. A buried AGN could be driving the radio luminosity, and it may not be appropriate to treat this CO nondetection in the context of star formation efficiencies and other related calculations.

2. We conclude that the radio luminosities of these SFRGs are higher for their overall mass than for the SMGs (given that if the radio SFRs are overestimated for one class, they could well be for both).

3. We note that SMGs in general and also these SFRGs are outliers of the stellar mass–SFR correlation (Daddi et al. 2007a), probably due to the higher efficiency in forming stars for a similar stellar mass and CO luminosity. Lower gas masses in the SFRGs would imply even higher SFEs than the SMGs. By contrast, if the SFRs are significantly overestimated by the radio, or the CO-to- H_2 conversion were significantly different from SMGs, then SFRGs could have efficiencies similar to typical ULIRGs. Together with the apparent low-efficiency star-forming (U)LIRGs from Daddi et al. (2008), the SMGs and SFRGs with SFRs several to 10 times larger than the Daddi et al. galaxies suggest roughly equal numbers of stars being formed in both high- and low-efficiency modes at $z \sim 2$. Massive galaxies are being built in an impressive variety of modes in the $z = 1$ – 3 peak star formation period.

4. If the radio-inferred SFRs are correct, then these SFRGs are more efficient star formers than SMGs and cannot be obviously interpreted as *scaled up* versions of local ULIRGs, as Tacconi et al. (2006, 2008) have argued is the case for SMGs. The SFRGs’ radio luminosities are larger than would naturally scale from local

ULIRGs given the gas masses or gas fractions. These observed gas masses and star formation properties may be typical of the SFRG population, and further work is justified to explore this population with improved statistics.

5. Our results underscore the fact that ultraluminous galaxies in the high-redshift universe have been discovered with a wide range of star-forming efficiencies, the SFRGs apparently being one extreme. Massive galaxies are likely being built in a variety of modes in the $z = 1-3$ peak star formation period.

We thank an anonymous referee for a very careful reading and helpful comments. This work is based on observations carried out with the IRAM Plateau de Bure Interferometer. IRAM is supported by INSU/CNRS (France), MPG (Germany), and IGN (Spain). S. C. C. acknowledges a fellowship from the Canadian Space Agency and an NSERC discovery grant. I. S. acknowledges support from the Royal Society. A. M. S. acknowledges support from STFC. We acknowledge the use of GILDAS software (see <http://www.iram.fr/IRAMFR/GILDAS>).

REFERENCES

- Alexander, D. M., Bauer, F. E., Chapman, S. C., Smail, I., Blain, A. W., Brandt, W. N., & Ivison, R. J. 2005, *ApJ*, 632, 736
- Baker, A. J., Tacconi, L. J., Genzel, R., Lehnert, M. D., & Lutz, D. 2004, *ApJ*, 604, 125
- Barger, A. J., Cowie, L. L., & Richards, E. A. 2000, *AJ*, 119, 2092
- Barger, A. J., Cowie, L. L., Sanders, D. B., Fulton, E., Taniguchi, Y., Sato, Y., Kawara, K., & Okuda, H. 1998, *Nature*, 394, 248
- Barger, A. J., Cowie, L. L., & Wang, W.-H. 2007, *ApJ*, 654, 764
- Baugh, C. M., Lacey, C. G., Frenk, C. S., Granato, G. L., Silva, L., Bressan, A., Benson, A. J., & Cole, S. 2005, *MNRAS*, 356, 1191
- Biggs, A. D., & Ivison, R. J. 2006, *MNRAS*, 371, 963
- . 2008, *MNRAS*, 385, 893
- Blain, A. W. 1999, *MNRAS*, 309, 955
- Blain, A. W., Smail, I., Ivison, R. J., Kneib, J.-P., & Frayer, D. T. 2002, *Phys. Rep.*, 369, 111
- Borys, C., Chapman, S., Halpern, M., & Scott, D. 2003, *MNRAS*, 344, 385
- Borys, C., Smail, I., Chapman, S. C., Blain, A. W., Alexander, D. M., & Ivison, R. J. 2005, *ApJ*, 635, 853
- Carilli, C. L., & Wang, R. 2006, *AJ*, 132, 2231
- Casey, C., et al. 2008a, *MNRAS*, submitted
- . 2008b, *MNRAS*, submitted
- Chapman, S. C., Blain, A., Ivison, R. J., & Smail, I. R. 2003a, *Nature*, 422, 695
- Chapman, S. C., Blain, A. W., Smail, I., & Ivison, R. J. 2005, *ApJ*, 622, 772
- Chapman, S. C., Lewis, G. F., Scott, D., Borys, C., & Richards, E. 2002, *ApJ*, 570, 557
- Chapman, S. C., Richards, E. A., Lewis, G. F., Wilson, G., & Barger, A. J. 2001, *ApJ*, 548, L147
- Chapman, S. C., Smail, I., Blain, A. W., & Ivison, R. J. 2004a, *ApJ*, 614, 671 (C04)
- Chapman, S. C., Smail, I., Windhorst, R., Muxlow, T., & Ivison, R. J. 2004b, *ApJ*, 611, 732
- Chapman, S. C., et al. 2000, *MNRAS*, 319, 318
- . 2003b, *ApJ*, 585, 57
- Coppin, K. E. K., et al. 2007, *ApJ*, 665, 936
- Daddi, E., Dannerbauer, H., Elbaz, D., Dickinson, M., Morrison, G., Stern, D., & Ravindranath, S. 2008, *ApJ*, 673, L21
- Daddi, E., et al. 2007a, *ApJ*, 670, 156
- . 2007b, *ApJ*, 670, 173
- Dale, D. A., & Helou, G. 2002, *ApJ*, 576, 159
- Dale, D. A., Helou, G., Contursi, A., Silbermann, N. A., & Kolhatkar, S. 2001, *ApJ*, 549, 215
- Desai, V., et al. 2006, *ApJ*, 641, 133
- Dowell, C. D., et al. 2003, *SPIE*, 4855, 73
- Greve, T. R., et al. 2005, *MNRAS*, 359, 1165
- Haarsma, D. B., & Partridge, R. B. 1998, *ApJ*, 503, L5
- Hainline, L. J., et al. 2008, *ApJ*, in press
- Helou, G., Soifer, B. T., & Rowan-Robinson, M. 1985, *ApJ*, 298, L7
- Hinshaw, G., et al. 2008, *ApJS*, in press (arXiv: 0803.0732)
- Houck, J., et al. 2005, *ApJ*, 622, L105
- Hughes, D. H., et al. 1998, *Nature*, 394, 241
- Ivison, R. J., et al. 2002, *MNRAS*, 337, 1
- . 2007a, *ApJ*, 660, L77
- . 2007b, *MNRAS*, 380, 199
- Kennicutt, R. C., Jr. 1998, *ApJ*, 498, 541
- Kneib, J.-P., Neri, R., Smail, I., Blain, A., Sheth, K., van der Werf, P., & Knudsen, K. K. 2005, *A&A*, 434, 819
- Kovacs, A., Chapman, S. C., Dowell, C. D., Blain, A. W., Ivison, R. J., Smail, I., & Phillips, T. G. 2006, *ApJ*, 650, 592
- Menendez-Delmestre, K., et al. 2007, *ApJ*, 655, L65
- Muxlow, T. W. B., et al. 2005, *MNRAS*, 358, 1159
- Neri, R., et al. 2003, *ApJ*, 597, L113
- Pope, A., et al. 2006, *MNRAS*, 370, 1185
- . 2008, *ApJ*, 675, 1171
- Richards, E. A., Fomalont, E. B., Kellermann, K. I., Windhorst, R. A., Partridge, R. B., Cowie, L. L., & Barger, A. J. 1999, *ApJ*, 526, L73
- Sajina, A., et al. 2008, *ApJ*, 683, 659
- Scott, S. E., et al. 2002, *MNRAS*, 331, 817
- Seaquist, E., Yao, L., Dunne, L., & Cameron, H. 2004, *MNRAS*, 349, 1428
- Smail, I., Ivison, R. J., & Blain, A. W. 1997, *ApJ*, 490, L5
- Solomon, P. M., Downes, D., Radford, S. J. E., & Barrett, J. W. 1997, *ApJ*, 478, 144
- Solomon, P. M., & Vanden Bout, P. A. 2005, *ARA&A*, 43, 677
- Swinbank, A. M., Chapman, S. C., Smail, I., Lindner, C., Borys, C., Blain, A. W., Ivison, R. J., & Lewis, G. F. 2006, *MNRAS*, 371, 465
- Swinbank, A. M., Smail, I., Chapman, S. C., Blain, A. W., Ivison, R. J., & Keel, W. C. 2004, *ApJ*, 617, 64
- Tacconi, L. J., et al. 2006, *ApJ*, 640, 228
- . 2008, *ApJ*, 680, 246
- Takata, T., Sekiguchi, K., Smail, I., Chapman, S. C., Geach, J. E., Swinbank, A. M., Blain, A., & Ivison, R. J. 2006, *ApJ*, 651, 713
- Valiante, E., Lutz, D., Sturm, E., Genzel, R., Tacconi, L. J., Lehnert, M. D., & Baker, A. J. 2007, *ApJ*, 660, 1060
- Weedman, D. W., Le Flo'c'h, E., Higdon, S. J. U., Higdon, J. L., & Houck, J. R. 2006a, *ApJ*, 638, 613
- Weedman, D. W., et al. 2006b, *ApJ*, 651, 101
- Yan, L., et al. 2005, *ApJ*, 628, 604
- . 2007, *ApJ*, 658, 778
- Yun, M. S., Reddy, N. A., & Condon, J. J. 2001, *ApJ*, 554, 803